17 April 1980

LETTER OF INTENT

DEEP INELASTIC WEAK AND ELECTROMAGNETIC INTERACTIONS OF MUONS

Bologna-CERN-Chicago-Dubna-Munich-Saclay-Wisconsin Collaboration

ABSTRACT

It is intended to continue at the Tevatron the investigation of deep inelastic muon scattering using an upgraded version of the NA4 spectrometer now in operation at the CERN-SPS.

The accurate determination of the nucleon structure functions over a large Q^2 range, up to 400 GeV^2 on H_2 and D_2 are made possible by the distributed target structure of the NA4 spectrometer. In addition the use of heavier targets and the increased muon energy available at the Tevatron will permit to study the effects of the weak interactions of muons through the γ-Z^0 interference and thus to measure the muon neutral current couplings.

THE COLLABORATION COMPOSITION

The list of the present NA4 participants is as follows:

D. BOLLINI, P.L. FRABETTI, G. HEIMAN, L. MONARI and F.L. NAVARRIA
Istituto di Fisica dell'Università, Bologna, Italy, INFN-Sezione di Bologna

A.C. BENVENUTI, M. BOZZO, R. BRUN, H. GENNOW, M. GOOSSENS, R. KOPP and L. PIEMONTESE
European Organization for Nuclear Research, CERN, Geneva, Switzerland

D. BARDIN, J. CVACH, N. FADEEV, I. GOLUTVIN, V. ILUSHCHENKO, I. IVANCHENKO, Y. KIRYUSHIN, V. KISSELEV, V. KHAVAROV, M. KLEIN, A. KONDOR, V. KRIVOKHIZHIN, V. KUKHTIN, I. MANNO, W. NOWAK, I. SAVIN, M. SHAFRANOVA, G. SMIRNOV, D. SMOLIN, P. TODOROV, G. VESZTERGOMBI, A. VOLODKO, A. ZARUBIN and J. ZACEK
Joint Institute for Nuclear Research, Dubna, USSR

D. JAMNIK, U. MEYER-BERKHOUT, A. STAUDE, K.M. TEICHERT, R. TIRLER, R. VOSS and C. ZUPANCIC
Section Physik der Universität, München, FRG

J. FELTESSE, A. LEVEQUE, J. MALASOMA, A. MILSZTAJN, G. SMADJA, Y. SACQUIN, M. VIRCHAUX, P. VERRECCHIA
CEN, Saclay, France

A substantial part of the present NA4 participants, including many senior physicists, have a strong interest in the future Tevatron experiments.

The participants from the USA laboratories include:

K.J. ANDERSON and J. PILCHER
University of Chicago, Chicago, Illinois

U. CAMERINI, D. REEDER and R. LOVELESS
University of Wisconsin, Madison, Wisconsin

Still, we believe that a strong participation of USA physicists, especially from Fermilab, is mandatory for the success of the experiment at the Tevatron. We would therefore welcome additional collaborators.

A. Benvenuti, CERN, will serve as contact person for communications concerning this letter of intent.

1. INTRODUCTION

By the time of muon deep inelastic scattering measurements at the Fermilab Tevatron ($\sim$ 1984) one can reasonably expect a number of related experiments performed. These include:

i) a measurement of inelastic nucleon structure functions $F_1(x,Q^2)$ and $F_2(x,Q^2)$ with a precision of a few percent in the regions $0.1 < x < 0.8$, $10 < Q^2 < 250$ GeV^2 for nuclear targets, and $10 < Q^2 < 150$ GeV^2 for H_2/D_2 targets;

ii) a first measurement of the beam charge asymmetry in μN scattering due to weak electromagnetic interference effects together with measurements of the radiative corrections;

iii) a measurement of the forward-backward asymmetry in $e^+e^- \rightarrow \mu^+\mu^-$ to provide the product of electron and muon axial coupling constants $a_e a_\mu$;

iv) a measurement of Z^0 production and decay via $Z^0 \rightarrow \mu^+\mu^-$, if indeed the Z^0 exists with the expected properties. Such a measurement provides the sum of squares of the vector and axial vector muon coupling $v_\mu^2 + a_\mu^2$.

Despite these results a number of questions will remain open which would benefit from the increased energy and duty cycle of the Tevatron. These include:

i) structure functions behaviour at low x, high Q^2 where the present kinematic limit raises serious doubts on the applicability of QCD due to higher twist effects;

ii) the extension of structure function measurements to the highest Q^2 available (high x) in order to probe the nucleon at shorter distances. Since the additional Q^2 span is only a factor of 2, precision will be of utmost importance and sensitive measurements with both H_2/D_2 and nuclear targets will be needed;

iii) a measurement of parity violating asymmetries which exploit the beam polarization and the fact that the asymmetries are expected to increase linearly with Q^2. The measurement of all the asymmetries will give a determination of muon coupling constants and a further test of μe universality.

We believe that careful measurements of these effects justify a program of muon scattering at the Tevatron and, as detailed below, an upgraded version of the NA4 spectrometer now running at the CERN-SPS is very well suited to these studies due to its unique characteristics:

(a) Ability to use 45 meter long hydrogen and deuterium targets for the measurement of the nucleon structure functions.

(b) Good resolution in Q^2 ($\Delta Q^2/Q^2 \sim 5\%$) and momentum ($\Delta p/p \sim 8\%$).

(c) Acceptance essentially independent of beam energy.

(d) Good Q^2 selectivity at the triggering level.

(e) Azimuthal detector symmetry which minimizes the dependence of the acceptance on the beam phase space and thus facilitates the measurements of the asymmetries $A^{\pm}$ and B (see sect. 4)

Even in the initial phase of the Tevatron running a typical run of $3 \cdot 10^{12}$ μ^+ at 550 GeV would give better than 3% statistical accuracy up to $Q^2 \sim 400$ GeV^2 using the hydrogen target and would cover the kinematical region from Q^2 of 30 to 400 GeV^2 and down to 0.05 in x.

The expected accuracy on the measurement of $A^{\pm}$ and B (see sect. 4) depends on the careful optimization of the beam intensity and polarization versus beam energy for a given amount of protons on target.

A realistic run of $3 \cdot 10^{12}$ each μ^+ and μ^- at 550 GeV on a carbon target would provide a measurement of the Q^2 and y dependence of the asymmetry parameter B with a typical error of $\sim 15\%$. A similar run for the asymmetry A^+ would yield an accuracy of $\sim 15\%$ at Q^2 of 200 GeV^2.

It is important to notice that the experience already achieved during the running at the SPS would ensure that accurate and reliable measurements could be performed from the very beginning of data taking at the Tevatron.

Finally we wish to point out that in designing the muon beams it is important to maintain the control of the beam polarization (i.e. pion and muon momenta controlled independently). This polarization control is a unique feature of the muon beams and is necessary for the study of the $\gamma - Z^0$ interference effects.

For a number of reasons we are not yet prepared to submit a full proposal with its implied commitment to a time table and funding pattern. The completion date of the muon program at CERN is not yet clearly enough in view. The principal work remaining is to use H_2/D_2 targets. While we estimate two years for completion of this work it is difficult now to be committed to a date for removal of the detector. At present the timing of the Tevatron Phase II is uncertain. Although 1984 has been established as the target date for beginning μ-scattering studies we understand that the detailed design study has not yet been issued and that explicit funding has not yet been approved. Finally, the technical details of the detector upgrade, transportation and its funding are not yet settled.

This letter of intent contains a description of the upgraded version of the spectrometer and the performance figures for the studies outlined above.

2. EXPERIMENTAL APPARATUS

The NA4 apparatus consists of a long target surrounded by a focusing spectrometer. This design, illustrated in fig. 1, is particularly suited to provide the high luminosity required to study deep inelastic muon scattering at very high Q^2 on hydrogen and deuterium targets.

The properties of this system are:

(a) Scaling invariance

The sagitta Δ of the muon in the toroid is approximately given by

$$\Delta = \frac{M_p}{0.3B} \frac{Q^2}{Q^2_{max}}$$ the units are: GeV., tesla, meters

hence for a given toroid radius the spectrometer will always confine a fixed percentage of the maximum Q^2 available, independently of the beam energy.

(b) Q^2 Selectivity

The Q^2 range of the trigger is determined simply by requiring that the μ had an excursion greater than Δ_{min} in the toroid. This is of great importance in order to obtain high statistics at high Q^2 due to the $1/Q^4$ fall off of the cross section.

These unique features make the NA4 spectrometer readily adaptable to the muon energy increase afforded by the Fermilab Tevatron.

2.1 SPS configuration

In more details the existing NA4 experiment, shown in fig. 2(a), consists of beam defining hodoscopes, a veto wall which eliminates the halo muons, the target spectrometer and the end detector.

The spectrometer is made of ten identical iron toroids (supermodules) with interspersed liquid scintillator counters and multiwire proportional chambers to detect and track the scattered muon.

The toroids provide a field which varies from 2.1 T at the center to 1.7 T at the outer edge. A five meter long target is housed in the central hole of each toroid. Three target types are available: hydrogen, deuterium and carbon.

Each supermodule, see fig. 2(b), is composed of eight modules each comprising four iron discs 110 mm thick with outer diameter of 275 cm and inner diameter of 50 cm spaced by 10 mm gaps.

With these dimensions and taking into account the dilution in bending power introduced by the air gaps, the spectrometer can contain 50% of the maximum Q^2 attainable at any given beam energy. Higher Q^2 can still be measured albeit with poorer resolution.

MWPC planes (two chambers/plane) each measuring one spatial coordinate with ± 2 mm accuracy are inserted after each module while the trigger counters are located every four modules.

The chambers are rectangular in shape with dimensions 1.5 m x 3 m and a central hole to allow for the passage of the beam.

The trigger counters are semi-circular and are subdivided into seven half-rings spanning uniformly from an inner diameter of 58 cm to an outer diameter of 270 cm. The light is collected at both ends of the half-rings and the PM pulses are sent after discrimination to mean timers to minimize the time variation due to the different impact points of the muon in the counter.

A set of five beam defining hodoscopes with a mosaic structure, designed to withstand fluxes of up to 10^9 muons/burst are installed in the spectrometer. They are used to correlate the beam muon which initiated the trigger with the momentum defining hodoscopes installed in the beam line and to the target section where the interaction occurred. The time of flight of each element of the hodoscopes is measured with an accuracy of one-half nanosecond at the occurrence of each trigger. Furthermore, they are used to monitor the beam flux and the steering of the beam through the apparatus, which is very important given the length of the spectrometer. The first of these hodoscopes is also used as "beam counter" in the trigger logic.

A bending magnet with bending power of 7 Tm is situated at the end of the spectrometer and is used to deflect the muons which have undergone a low Q^2 interaction ($Q^2 < 4(GeV/c)^2$) into a muon identifier 25 m downstream (End Detector). The End Detector accepts muons within 30 - 130 GeV/c, at 280 GeV incident beam energy.

2.2 Tevatron Configuration

The physics program to be pursued at the Tevatron requires high accuracy both in statistics and systematics. It is therefore important that the same experiment covers as much of the Q^2, x domain as possible.

The NA4 spectrometer is essential to investigate the high Q^2 and hence high x region where the event rates are very small. The low x region is not properly covered by the spectrometer, however, here the event rates are sufficiently high that only a single target section is required. Based on the experience gained running at SPS energies, we show in fig. 3 the configuration of the apparatus we are considering for the Tevatron. A target section is located 20 m upstream of the first supermodule and is followed by a system of multiwire proportional chambers and segmented trigger counters to select events originating in this target and measure the muon direction before it enters the toroid.

This upstream spectrometer will measure muon scattering angles from 0.8 to 3 degrees and nicely complements and overlaps the region investigated by the existing spectrometer. Smaller scattering angles can be investigated during dedicated runs in which some of the supermodules have been removed from the beam line. The supermodules are disposed with $\sim$ 2 m gaps to allow for small angle chambers to be inserted between supermodules. These chambers will provide a measurement of the muon angle before the magnetic detection and will improve the momentum fit at low Q^2. We foresee to have an end detector to tag the very low Q^2 events which could produce background events in the spectrometer by leptonic decays in the hadron shower. The region of the $Q^2\nu$ plane accessible to this experiment at the Tevatron is shown in fig. 4 together with the region already investigated at the CERN SPS.

2.3 Spectrometer Resolution

The momentum resolution has been measured to be 8% rms from the energy spread of a 100 GeV muon beam displaced into the spectrometer. The resolution is independent of the muon momentum above $\sim$ 20 GeV/c.

The estimated Q^2 resolution varies from $\sim$ 5% at $Q^2/Q^2_{max} \simeq 0.4$ to about 10% at $Q^2/Q^2_{max} \simeq 0.1$ and deteriorates quickly for lower Q^2 values.

The main contribution to the error is due to the multiple scattering in the iron prior to the angular measurement. This becomes the limiting factor at low Q^2.

In the spectrometer configuration proposed for the Tevatron, the region with $Q^2/Q^2_{max} \lesssim 0.08$ is studied with the upstream target where the muon angle is determined prior to the momentum analysis. The estimated Q^2 resolution in this region is about 5%.

Similarly we expect to measure the muon angle at moderate Q^2 ($\simeq 0.1\ Q^2_{max}$) with the new small angle chambers which are located between the supermodules.

In this way the Q^2 resolution will be about 5% throughout the whole Q^2 range studied in this experiment.

2.4 The Distributed Trigger

The standard trigger used in the NA4 experiment is defined as the coincidence of four consecutive planes with a beam particle not accompanied by a halo particle. The Q^2 selectivity is obtained by changing the ring configuration in the trigger counters. In more details, the output of each half-ring in a trigger plane is combined by a remotely controlled OR unit to give a "plane signal". This information is then transmitted through a fast, rigid copper conductor called a high-way ($\beta = 0.99$) to the neighbouring supermodules. The trigger is then configured independently at each supermodule by sampling the information from six consecutives counter planes which is available synchronously with the beam and halo information via the fast high-way. Upon occurrence of a trigger a strobe signal is generated and distributed to the chambers of each supermodule via the high-way.

The triggering rate with a 40 m carbon target is typically of 8 10^{-6} per gated μ at 200 GeV with Q^2 greater than 35 GeV/c^2. The trigger composition consists of 65% of hadron showers penetration from low Q^2 interactions (see fig. 5), 15% of halo induced events, 20% good events (see fig. 6).

Using this triggering scheme at the Tevatron we expect for the same target the following triggering rates:

- low Q^2 trigger ($Q^2 > 60$ GeV^2) $\sim 2 \cdot 10^{-4}$/Gated μ
- high Q^2 trigger ($Q^2 > 100$ GeV^2) $\sim 1.2 \cdot 10^{-5}$/Gated μ with $E_\mu = 550$ GeV

The triggering rate can be reduced by a factor of ten by performing a second level logic based on the multiplicity of wire hits in the MWPC's without any loss of good events.

3. DEEP INELASTIC ELECTROMAGNETIC INTERACTIONS

3.1 Physics motivations

The pioneer experiments [1] performed at SLAC on deep inelastic electron scattering confirmed within 20% the scaling hypothesis proposed by Bjorken [2]. Subsequent experiments [3] at SLAC and Fermilab with muon beams found evidence for departures from this naive model and established the dependence of the structure functions on Q^2.

Quantum chromodynamics (QCD) [4] makes definite predictions on the Q^2 dependence of the structure functions and their moments that can be directly tested by deep inelastic scattering data.

The initial successes of the theory in correctly predicting the $1/(\ell n\ Q^2/\Lambda^2)$ dependence of the structure function moments have been recently reassessed [5]. It has been in fact realized that corrections to the leading order term in the form of powers of $1/Q^2$ (higher-twists) must be included in the analysis. This in turn introduces uncertainties in the determination of the scale parameter Λ and thus vitiates the test of the theory.

Given the difficulty in calculating the bound state effects in the nucleon substructure which determine these higher twist terms it is mandatory to have precise data over as large a Q^2-x region as possible.

The second generation experiments on deep inelastic muon scattering at the CERN-SPS (NA2, NA4) will provide in the near future data of sufficient quality to test the theory. However the crucial low x, high Q^2 region will be vitally extended by the increase in muon energy afforded by the Tevatron.

Another stringent test of QCD will be provided by a good determination of the parameter $R = \sigma_L/\sigma_T$. Present data are not of sufficient accuracy to constraint the theory which predicts a value of R systematically lower than the observed one.

These developments in our understanding of the nucleon structure functions point out the need for accurate and systematic studies of deep inelastic muon scattering on hydrogen and deuterium targets over the largest Q^2 range possible. The use of the same spectrometer over beam energies from 100 to 800 GeV would assure the internal consistency of the data necessary to unravel the QCD predictions.

3.2 Event rates

The detailed strategy of the data taking cannot be formulated at this time since it depends on the performance of the muon beam to be built at the Tevatron and on the results of the NA4 running at the CERN SPS.

As an illustration of the potentiality of the detector we plot in figs. 7 and 8 the events accumulated in the spectrometer above a given Q^2 during a typical running period in the initial phase of the Tevatron operation.

The parameters used for this calculation are [6]

Beam Energy	550 GeV
Interacting protons/pulse	$6\ 10^{12}$
Muons/pulse	$1.6\ 10^{8}$
Running time	300 hours
Total flux	$3 \cdot 10^{12}$ muons
Target	40 m H_2
External target	5 m H_2

This run would yield several thousand events with $Q^2 \geqslant 400\ GeV^2$. In addition we would also accumulate in the upstream hydrogen target 27 000 events with

$$0.05 \leqslant x \leqslant 0.1$$
$$35 \leqslant Q^2 \leqslant 80\ GeV^2$$

and 7500 events with

$$0.1 \leqslant x < 0.2$$
$$80 \leqslant Q^2 < 150\ GeV^2$$

The importance of precise measurements of deep inelastic cross sections at large Q^2 has triggered a comprehensive study [7] of other so called radiative processes and corresponding radiative corrections (RC) to the one-photon exchange process.

In fact the upper limit in the Q^2 range is determined by the requirement that the radiative corrections to the cross section be less than 30%. This implies a cut off on y at about 0.8.

4. WEAK INTERACTIONS OF MUONS

4.1 Cross sections and asymmetries

The observation by Novosibirsk [8] and SLAC [9] groups of the parity violating lepton-hadron interaction is one of the most important experimental results obtained in recent years.

These two experiments as well as the phenomenological analysis [10] of all neutrino neutral current data [11] show the overall agreement between the experiments and Weinberg-Salam (WS) theory within about 20% uncertainties. Further verification of the theory requires the study of a number of asymmetries in the deep inelastic scattering of longitudinally polarized high energy μ^+ and μ^- on nucleons which could confirm the expected Q^2-dependence of the effects increased by hundreds times at Tevatron energies in comparison with the SLAC ones. The complete measurement of asymmetries would provide a determination of the unknown muon weak neutral current couplings and a crucial check of WS theory.

The deep inelastic scattering of muons on nucleons to the lowest order in weak and electromagnetic interactions is represented by one photon and one Z^0 exchange diagrams.

The resulting cross sections in a first approximation will contain a γ-term and a $\gamma - Z^0$ interference term:

$$d\sigma \simeq d\sigma_{\gamma} + d\sigma_{\gamma Z^0} + \ldots$$

The contribution coming from the last term, $d\sigma_{\gamma Z^0}$, is given by the expression [12]

$$d\sigma^{\mp}_{\gamma Z}(\lambda) \equiv \frac{d^2\sigma^{\pm}_{\gamma Z}(\lambda)}{dQ^2 d\nu} = \frac{G}{\sqrt{2}} \cdot \frac{\alpha}{Q^2 \nu} \left\{ \left[1 + (1-y)^2 \right] G_2 (-v_{\mu} \pm \lambda a_{\mu}) \right.$$

$$\left. + \left[1 - (1-y)^2 \right] \times G_3 (\pm a_{\mu} - \lambda v_{\mu}) \right\}$$

where v_{μ}, a_{μ} represent the vector and axial coupling constants of the muon, G_2 and G_3 are new structure functions containing the quark couplings to Z^0-boson.

Neglecting the higher order electromagnetic and weak terms one can write the overall $\mu^{\mp}(\lambda)N \to \mu^{\mp}h$ cross section $d\sigma^{\mp}(\lambda)$ normalized to the electromagnetic term $d\sigma_0$

$$\frac{d\sigma^{\mp}(\lambda)}{d\sigma_0} = 1 - k \left[(v_\mu V \mp a_\mu A + \lambda(v_\mu A \mp a_\mu V) \right]$$

where V and A are ratios of structure functions:

$$V = \frac{G_2}{F_2}, \quad A = A_0 \cdot g(y) = \frac{xG_3}{F_2} \cdot \frac{1 - (1-y)^2}{1 + (1-y)^2}$$

and k is a constant determining the strength of γZ-interference effect:

$$k = \frac{G}{\sqrt{2}} \cdot \frac{Q^2}{2\pi\alpha M^2} = 1.79 \cdot 10^{-4} \cdot Q^2$$

From the overall cross sections one can derive the following experimentally observable asymmetries

$$A^{\mp}(\lambda_1,\lambda_2) = \frac{d\sigma^{\mp}(\lambda_1) - d\sigma^{\mp}(\lambda_2)}{d\sigma^{\mp}(\lambda_1) + d\sigma^{\mp}(\lambda_2)} = \begin{cases} -k \frac{\lambda_1-\lambda_2}{2} (\mp a_\mu V + v_\mu A), \\ -k\lambda(\mp a_\mu V + v_\mu A) \text{ for } \lambda_1 = -\lambda_2 \end{cases}$$

which are measured by varying the beam polarization without changing its sign; and

$$B(\lambda_1,\lambda_2) = \frac{d\sigma^{+}(\lambda_1) - d\sigma^{-}(\lambda_2)}{d\sigma^{+}(\lambda_1) + d\sigma^{-}(\lambda_2)} = \begin{cases} -k(a_\mu A + \frac{\lambda_1-\lambda_2}{2} v_\mu A - \frac{\lambda_1+\lambda_2}{2} a_\mu V) \\ -k(a_\mu - \lambda v_\mu)A \text{ for } \lambda_1 = -\lambda_2 \end{cases}$$

which is measured by varying both λ and muon charge. The measurement of the asymmetries A^{+}, A^{-} and B would provide a complete determination of all muon coupling constant combinations:

$$a_\mu V = \frac{1}{2k\lambda}\left[A^-(\lambda) - A^+(\lambda)\right]$$

$$v_\mu A = \frac{1}{2k\lambda}\left[A^-(\lambda) + A^+(\lambda)\right]$$

$$a_\mu A = -\frac{1}{k}\left[B(\lambda) + \tfrac{1}{2}(A^-(\lambda) + A^+(\lambda))\right].$$

Note that A^+ and A^- contain only the P-violating combinations. The asymmetry B contains P-violating combination $v_\mu A$ and P-conserving combination $a_\mu A$.

4.2 Estimation of the asymmetry effects

The estimation of the asymmetries $A^\pm$ and B values has been made assuming that muon couplings and their products with the structure function ratios are calculated from WS/GIM and QPM models for the WS-parameter $\sin^2\theta = 0.23$ [9-13]. Within these assumptions the above formulae became simpler:

$$A^- \simeq A^+ \simeq -k\,\frac{\Delta\lambda}{2}\,a_\mu V = \frac{-\Delta\lambda}{2} \cdot 0.72 \cdot 10^{-4} Q^2$$

i.e. almost y-independent and

$$B \simeq -0.5 \cdot k\, a_\mu A \simeq -1.61 \cdot 10^{-4} \cdot g(y) \cdot Q^2$$

i.e. almost λ-independent. This is illustrated in fig. 9.

The experimental conditions for the asymmetry measurements must be carefully optimized in order to take full advantage of the beam qualities and reach the most profitable compromise between Q^2-range and the achievable beam fluxes and polarizations.

A realistic running plan for the initial phase of Tevatron operation is outlined below:

Asymmetry	B	A^+
Beam energy	550 GeV	450 GeV
Total μ flux	$2 \times 3 \cdot 10^{12}$	$2 \times 3 \cdot 10^{12}$
Running time μ^+	300 hours	300 hours
Beam polarization	0.8	0.8
Running time μ^+		$\sim$ 900 hours
Beam polarization		- 0.2
Running time μ^-	$\sim$ 900 hours	
Beam polarization	- 0.8	

The expected asymmetries B and A^+ and their statistical accuracy obtainable under these conditions are shown in figs 10 and 11 respectively. The precision of the y dependence of A^+ is given in fig. 12.

At Q^2 values of about 400 $(GeV/c)^2$ and $\frac{1}{2}|\Delta\lambda| \simeq 0.5$ the expected value of the asymmetry $|A^{\pm}|$ is equal to about 1.5%, i.e. 150 times more than that measured at SLAC.

The asymmetry B in the same conditions and for $\bar{y} = 0.7$ will be about -5.5%.

In conclusion the asymmetries $|A^{\pm}|$ are considerably smaller than the asymmetry B and will require more careful experimental approach, control of possible systematic errors and better statistical precision than those given for asymmetry B at Tevatron energies.

However, it is feasible to plan on measuring at least A^+ and B in the initial phase of the Tevatron running. At the same time these data will provide accurate determination of the structure functions up to $Q^2 \simeq 700$ $(GeV/c)^2$ on carbon, see fig. 13.

Below we give a short summary of additional physical information that can be extracted from the measurements of all the asymmetries.

One can see from the general expressions for $A^{\pm}$ and B that at y = 0

$$A^- = - A^+$$

and

$$B/_{y=0} = 0$$

due to the kinematical property of $A/_{y=0} = 0$. These results are model independent and rely only on the V-A structure of the weak interaction Hamiltonian. Measurements of the y-dependence of the asymmetries and their extrapolation to y = 0 would provide a check of this hypothesis.

From the sum of A^- and A^+ we get

$$A^- + A^+ = -2kv_\mu A = -2k\ (-\tfrac{1}{2} + 2\ \sin^2\theta)A.$$

Using value of A from neutrino data we can determine the WS parameter $\sin^2\theta$ directly. Furthermore, we can avoid to use the value of A from neutrino experiments (or from QPM) by measuring B at two different beam polarization λ and λ' [13].

Note that $\sin^2\theta \equiv \sin^2\theta_\ell$ defined from the sum $A^+ + A^-$ or from B enters in the leptonic neutral current (v_μ). In the so called alternative Bjoken theory [14] it differs from $\sin^2\theta \equiv \sin^2\theta_h$ entering in hadronic neutral currents determined from neutrino data. In the WS theory $\sin^2\theta_\ell = \sin^2\theta_h$. For the determination of $\sin^2\theta_h$ from the measured asymmetries one can use the relation

$$A^- - A^+ \sim a_\mu V \sim \sin^2\theta_h.$$

These measurements would also give a very stringent test on possible right handed weak neutral currents [13].

4.3 Radiative corrections to the asymmetries

In the above considerations we have only taken into account the photon exchange contribution to the cross section and its interference with Z^0-boson exchange.

The contribution of other radiative processes and the corresponding radiative corrections (RC) to the asymmetries $A^{\pm}$ and B have been calculated [15] in the framework of WS theory and quark parton model. For details of the calculation we refer to the original paper. The results for a muon energy of 500 GeV are shown in fig. 14.

The radiative corrections to $A^{\pm}$ and B at fixed Q^2 and y depend only slightly on the muon energy. The size of RC's is not bigger than 10% for $A^{\pm}$ and reaches about 30% for B.

4.4 Systematic errors

A number of sources of possible systematic errors have been considered which can create artificial asymmetries in the determination of either the Q^2-dependence of $A^{\pm}$ and B or their absolute values. They include: (1) beam phase space, (2) uncertainty in the magnetic field setting and monitoring, (3) beam and apparatus stability. In the kinematic region of this measurement we see no limitations at the level of 1% (0.2% optimistically) from items (1) to (2). To minimize item (3) we need frequent reversals of the beam polarity and the same beam intensity must be maintained for μ^+ and μ^-.

To investigate systematic effects directly, a short test has been performed at CERN SPS using 200 GeV μ^+ and μ^- beams with a single polarity reversal. Data taken with the two polarities have been compared in a number of ways including the longitudinal position of the interaction vertex, the azimuthal angle, the momentum and polar angle of the scattered muon. Within the statistical accuracy of $\sim$ 2% there is no evidence of any systematic errors.

The NA4 experiment is now collecting data for the B asymmetry measurement at 200 GeV and expects to obtain the statistical precision shown in fig. 15.

REFERENCES

[1] E.D. Bloom et al., Phys. Rev. Lett. 23 (1969) 930;
E. Breidenbach et al., Phys. Rev. Lett. 23 (1969) 935;
G. Miller et al., Phys. Rev. D5 (1970) 528.

[2] J.D. Bjorken, Phys. Rev. Lett. 16 (1966) 408;
J.D. Bjorken, Phys. Rev. 179 (1969) 1547.

[3] R.F. Taylor, "Proceedings of the 1975 Symposium on Lepton and Photon Interactions at High Energies, Stanford, 1975;
Y. Watenabe et al., Phys. Rev. Lett. 35 (1975) 898;
C. Chang et al., Phys. Rev. Lett. 35 (1975) 901;
H.L. Anderson et al., Phys. Rev. Lett. 37 (1976) 4;
H.L. Anderson et al., Phys. Rev. Lett. 38 (1977) 1450;
B.A. Gordon et al., Phys. Rev. Lett. 41 (1978) 615.

[4] H.D. Politzer, Phys. Rev. Lett. 26 (1973) 1346 (see also)
H. D. Politzer, Phys. Rep. 14C (1974) and reference therein.

[5] L.F. Abbott and R.M. Barnett, Report No SLAC-PUB-2325 (May 1979) to be published in Annals of Physics;
L.F. Abbott, W.B. Atwood and R.M. Barnett, SLAC-PUB-2400 (September 1979) to be published in Phys. Rev. D.

[6] Muons Yields from "Design Study for a High Energy Muon Beam" R. Evans, T. Kirk and A. Malensek, Fermilab TM-754 (2960) and "Neutrino-Muon Workshop" by T.B. Kirk, Fermilab Report November 1979-8.

[7] D. Bardin et al., JINR preprints, Dubna P2-9940, G2-10147, G2-10205, 1976, G2-10471, P2-10872, P2-10873, 1977;
J. Drees, preprint WU-878-16, Wuppertal, 1978.

[8] L. Barkov, L. Zolotarev, Pisma JETF 27 (1978) 379.

[9] C.Y. Prescott et al., Phys. Lett. 77B (1978) 347 and Invited talk at the EPS Conference, Geneva, June 1979.

RERENCES (Cont'd)

[10] M. Ross and I. Liede, Phys. Lett. 82B (1979) 89;
L. Abbott and R.M. Barnett, Phys. Rev. D18 (1978) 3214;
M. Koruma, T. Oka, Prog. Theor. Phys. 60 (1978) 842;
M. Klein and T. Reimann, Berlin, PHE 78-10 (1978).

[11] P. Posetti et al., CERN Preprint 1978;
M. Holder et al., Phys. Lett. 72B (1977) 254;
K. Winter, "Review of Experimental Measurements of Weak Neutral Current Interactions", CERN/EP/79-132, 1979.

[12] M. Klein, "Muon-Induced Weak Neutral Currents", Ecole Internationale de Physique des Particules Elémentaires, Kupari-Dubrovnic (Yougoslavia, 1979).

[13] M. Klein, T. Rieman and I. Savin, Phys. Lett. 85B (1979) 385;
S.M. Bilenky, JINR Preprint, E2-12014 (1978) Dubna.

[14] J. Bjorken, SLAC-PUB-2146 (1978).

[15] D. Bardin et al., JINR Preprint, Dubna, E2-12761, E2-12564, 1979.

FIGURE CAPTIONS

Fig. 1 Principle of Q^2-focussing spectrometer.

Fig. 2 CERN SPS configuration of the NA4 set up (a) and the spectrometer supermodule structure (b).

Fig. 3 Tevatron set up configuration.

Fig. 4 A kinematical plot of muon-nucleon inelastic interactions and regions covered by the NA4 spectrometer.

Fig. 5 Display of a typical low Q^2 event.

Fig. 6 Display of a typical high Q^2 event.

Fig. 7 Event rates from hydrogen targets.

Fig. 8 Event rates from one external target.

Fig. 9 Weinberg-Salam theory predictions for the muon-nucleon cross section asymmetries.

Fig. 10 Estimations of the effect and statistical errors for the B-asymmetry measurements at E = 550 GeV.

Fig. 11 Estimations of the effect and statistical errors for the A^+-asymmetry measurements at E = 450 GeV.

Fig. 12 The expected accuracy of a y-dependence study of the $A^{\pm}$-asymmetry.

Fig. 13 Event rates from carbon targets.

FIGURE CAPTIONS (Cont'd)

Fig. 14 Asymmetries in the muon-nucleon deep inelastic cross sections in units $[10^2/(Q^2 GeV^{-2})]$ calculated from the one-photon and Z^0 exchange diagrams (dashed-dotted lines), all radiative diagrams (solid lines) and restricted set of RC diagrams (dashed lines) [15]:

(a) asymmetry $A^{\pm}$ at E = 500 GeV,

(b) asymmetry B at E = 500 GeV,

for fixed Q^2 indicated above the curves.

Fig. 15 Expected precisions for the asymmetry B measurement at CERN SPS.

PRINCIPLE OF q^2 - FOCUSSING SPECTROMETER

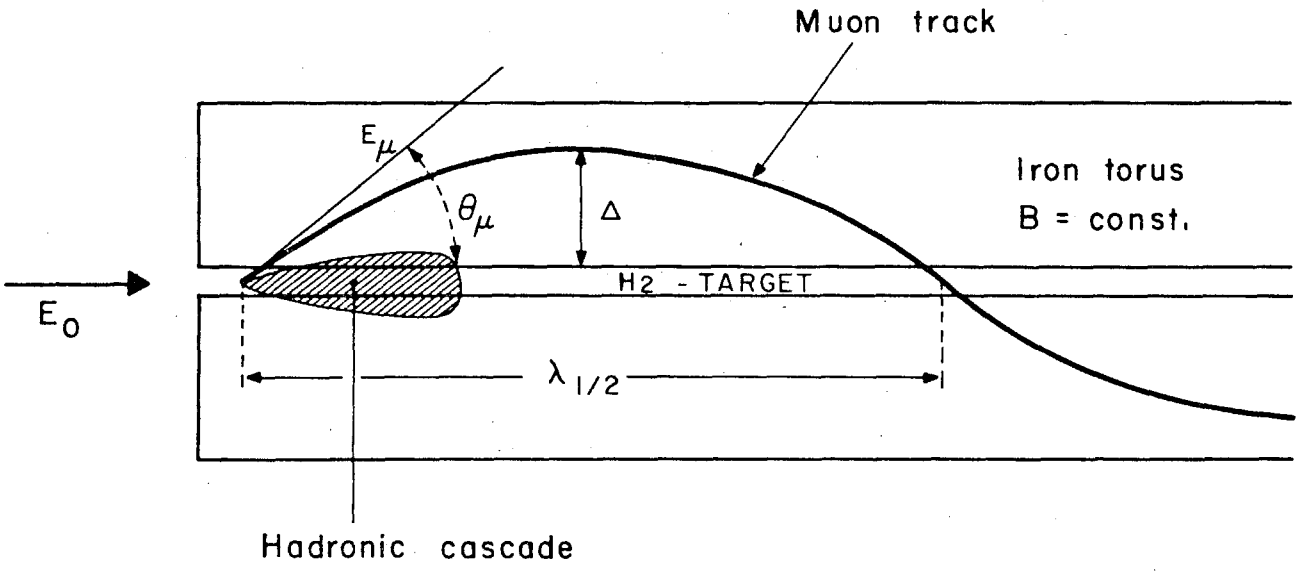

$$\lambda_{1/2} = 6.66\ p_\perp / B$$

$$\Delta = \frac{Mp}{0.3B} \quad \frac{q^2}{q^2_{max}}$$

fig. 1

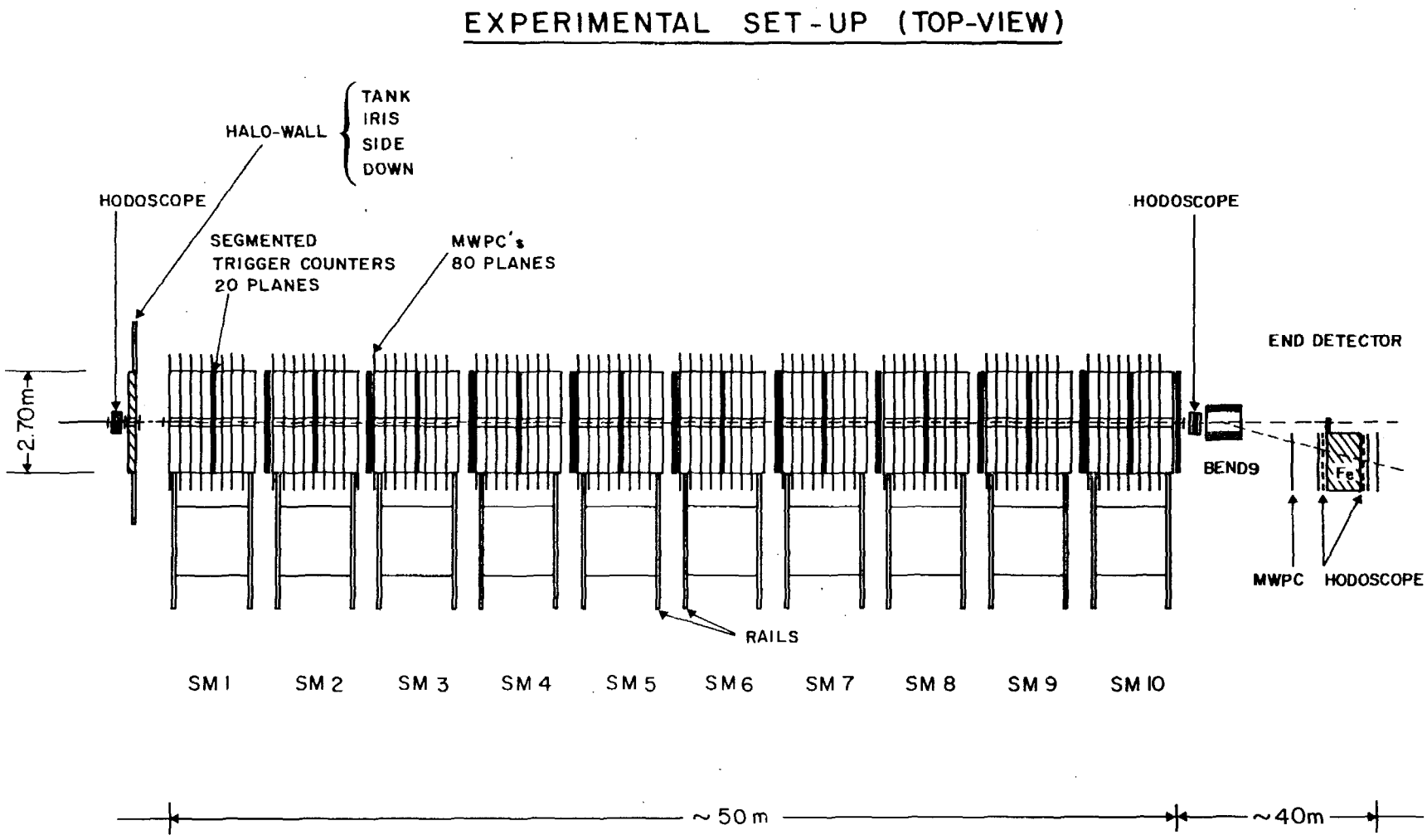
EXPERIMENTAL SET-UP (TOP-VIEW)
HALO-WALL
TANK
IRIS
SIDE
DOWN
HODOSCOPE
SEGMENTED
TRIGGER COUNTERS
20 PLANES
MWPC's
80 PLANES
HODOSCOPE
END DETECTOR
2.70m
BEND9
Fe
MWPC
HODOSCOPE
RAILS
SM 1
SM 2
SM 3
SM 4
SM 5
SM 6
SM 7
SM 8
SM 9
SM 10
~50m
~40m

fig. 2(a)

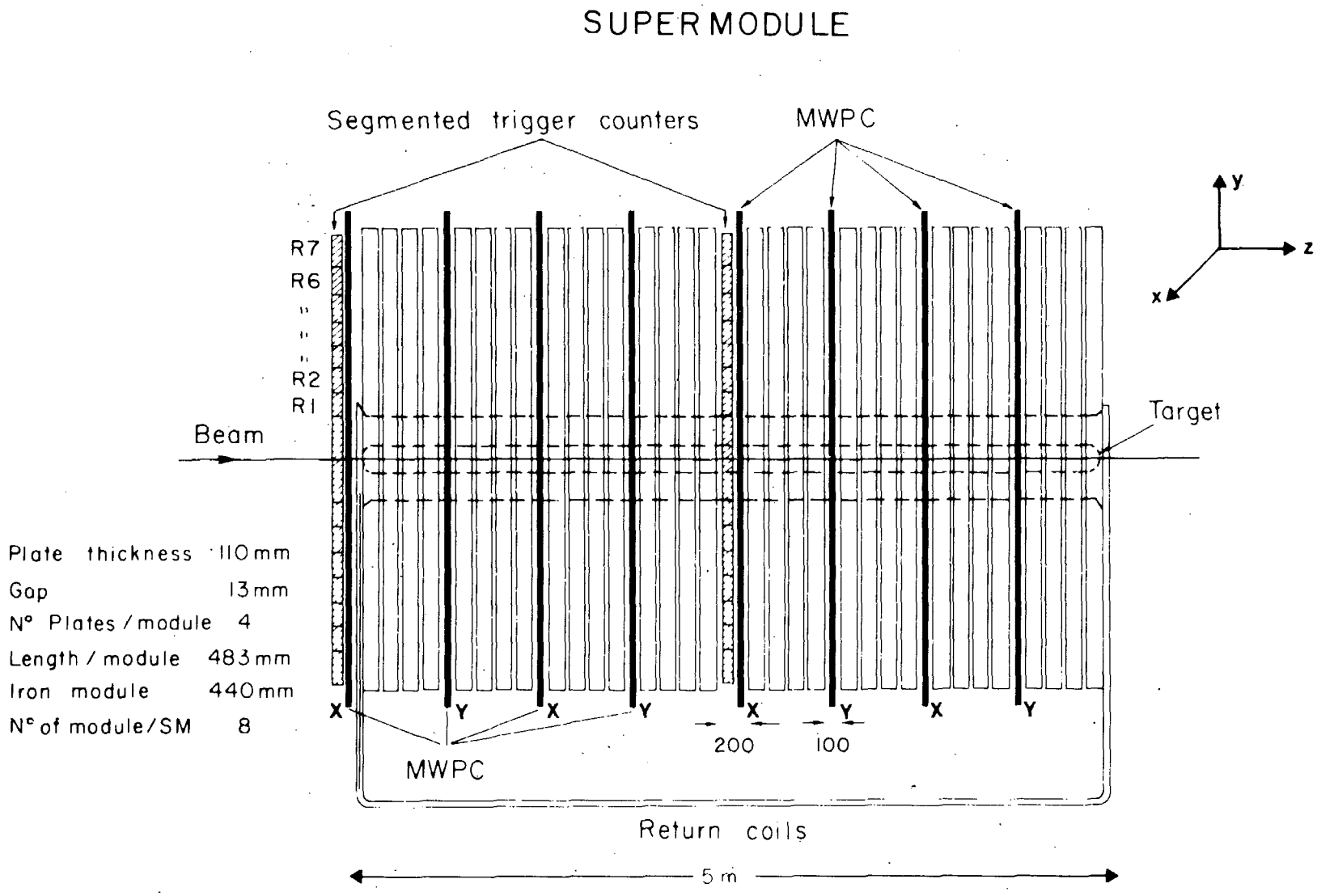
SUPER MODULE
Segmented trigger counters
MWPC
y
z
x
R7
R6
R2
R1
Beam
Target
Plate thickness 110 mm
Gap 13 mm
N° Plates / module 4
Length / module 483 mm
Iron module 440 mm
N° of module/SM 8
X
Y
X
Y
X
Y
X
Y
200
100
MWPC
Return coils
5 m

fig. 2(b)

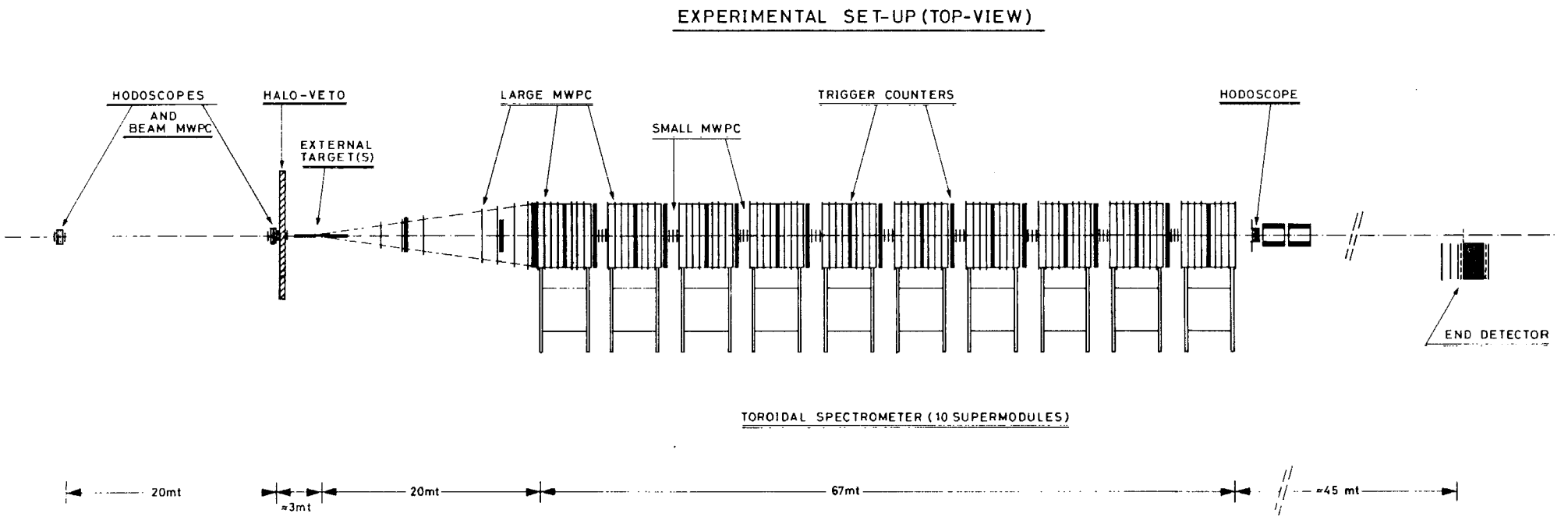
EXPERIMENTAL SET-UP (TOP-VIEW)
HODOSCOPES
AND
BEAM MWPC
HALO-VETO
EXTERNAL
TARGET(S)
LARGE MWPC
SMALL MWPC
TRIGGER COUNTERS
HODOSCOPE
END DETECTOR
TOROIDAL SPECTROMETER (10 SUPERMODULES)
20mt
≈3mt
20mt
67mt
≈45 mt

fig. 3

REGIONS COVERED BY THE NA-4 SPECTROMETER

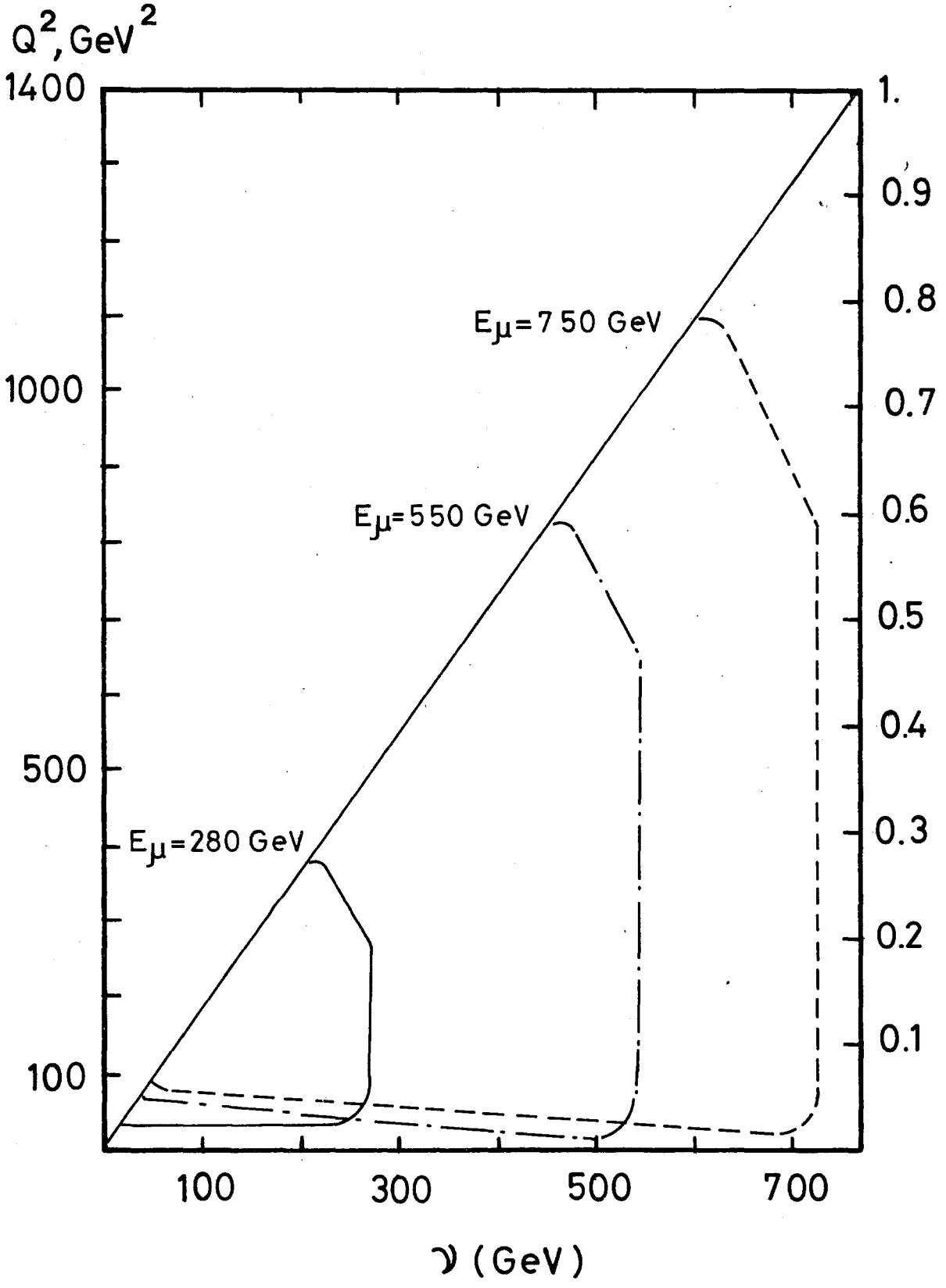

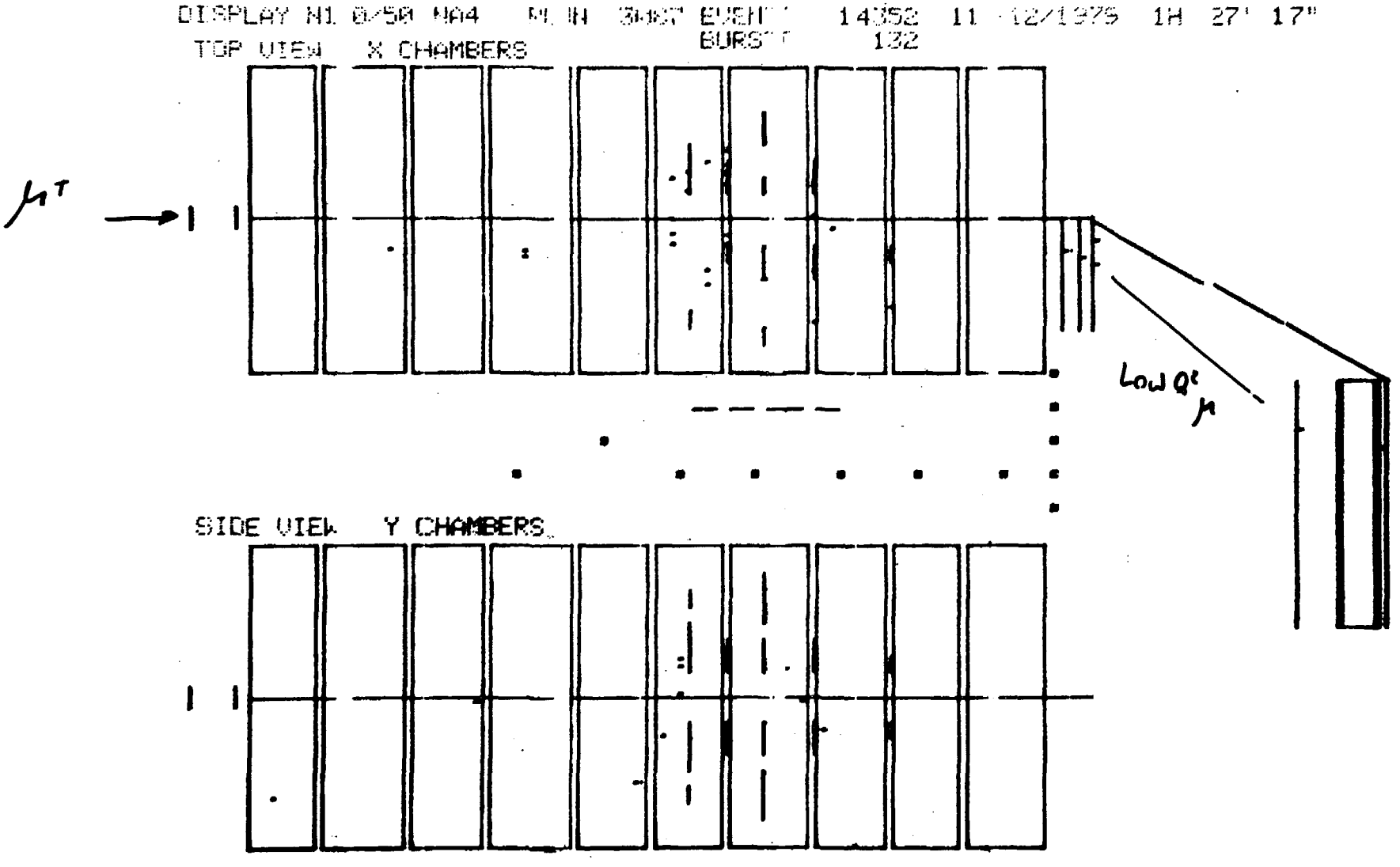

fig. 5

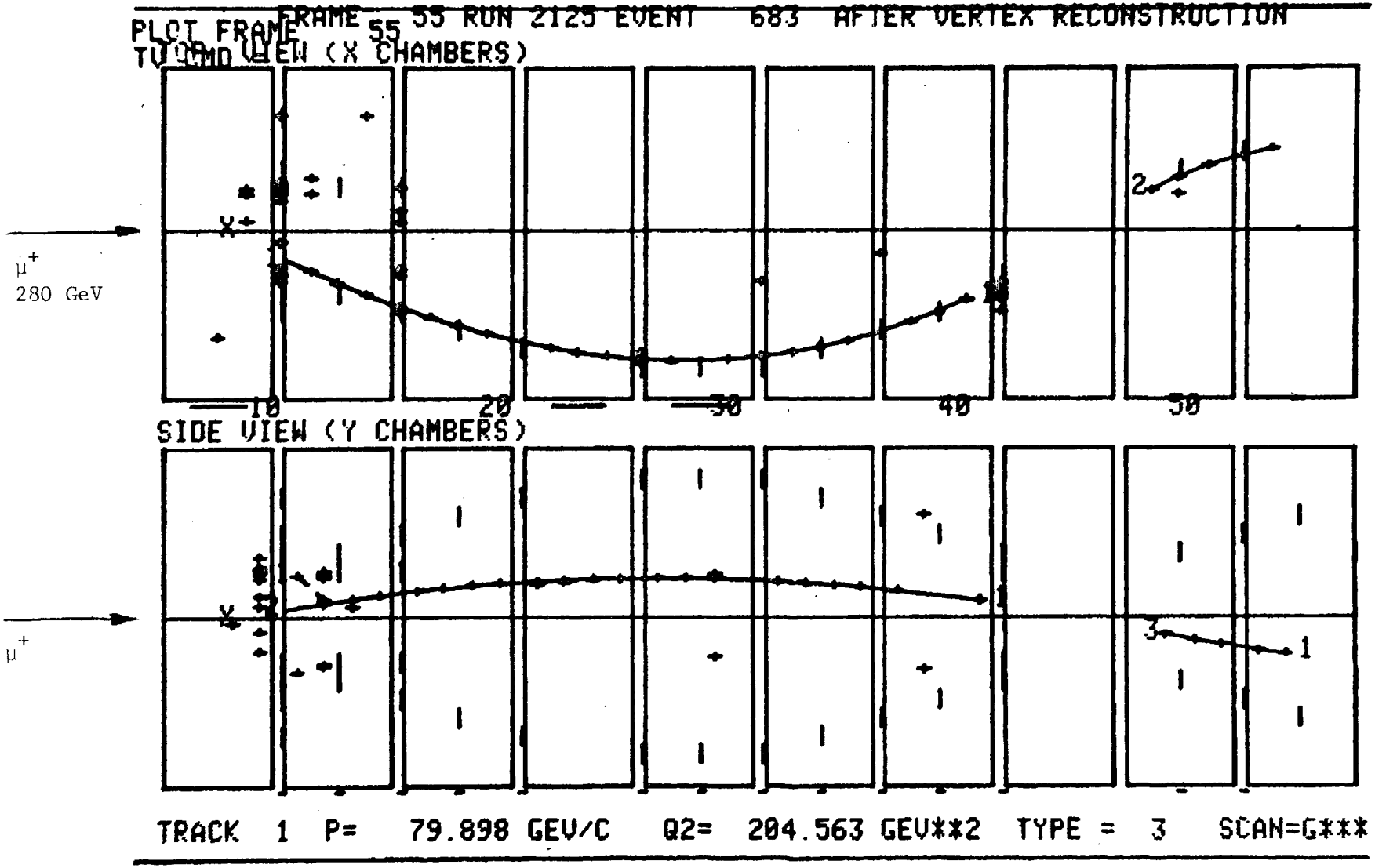
FRAME 55 RUN 2125 EVENT 683 AFTER VERTEX RECONSTRUCTION
PLOT FRAME 55
TOP VIEW (X CHAMBERS)
μ+
280 GeV
10
20
30
40
50
SIDE VIEW (Y CHAMBERS)
μ+
TRACK 1 P= 79.898 GEV/C Q2= 204.563 GEV**2 TYPE = 3 SCAN=G***

fig. 6

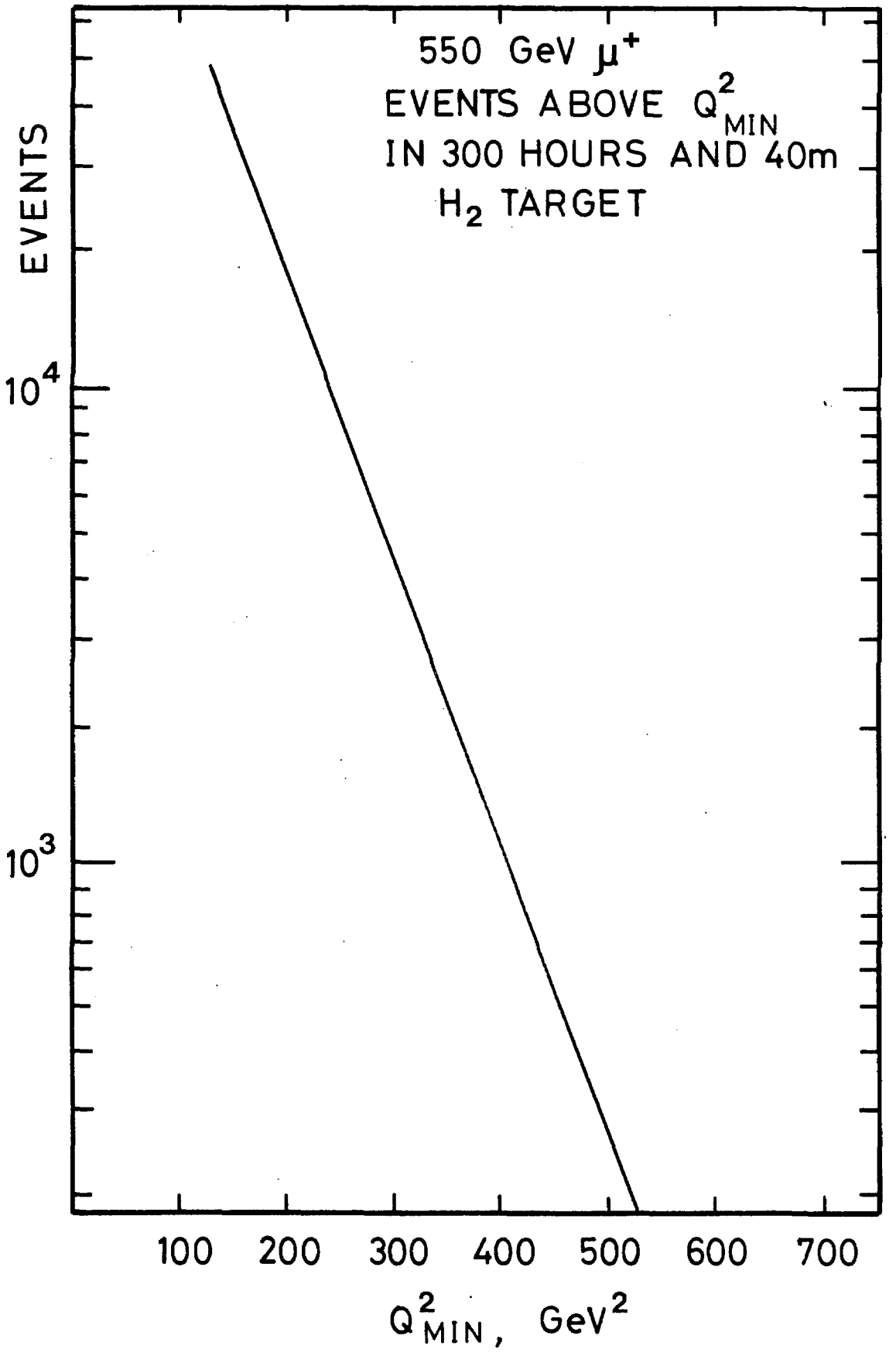
550 GeV μ+
EVENTS ABOVE Q²MIN
IN 300 HOURS AND 40m
H2 TARGET
EVENTS
10⁴
10³
100
200
300
400
500
600
700
Q²MIN, GeV²

fig. 7

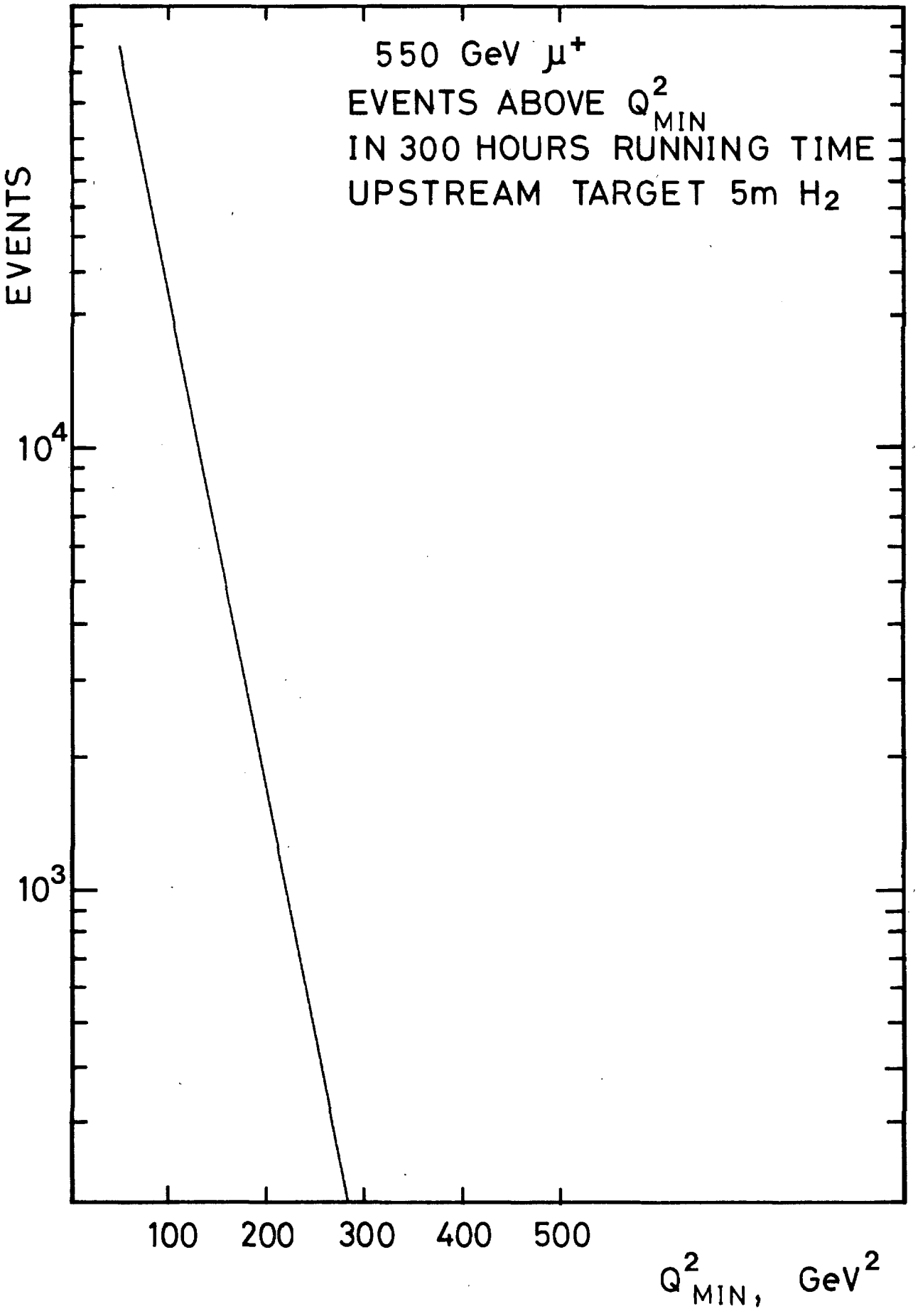
550 GeV μ+
EVENTS ABOVE Q²MIN
IN 300 HOURS RUNNING TIME
UPSTREAM TARGET 5m H2
EVENTS
10⁴
10³
100
200
300
400
500
Q²MIN, GeV²

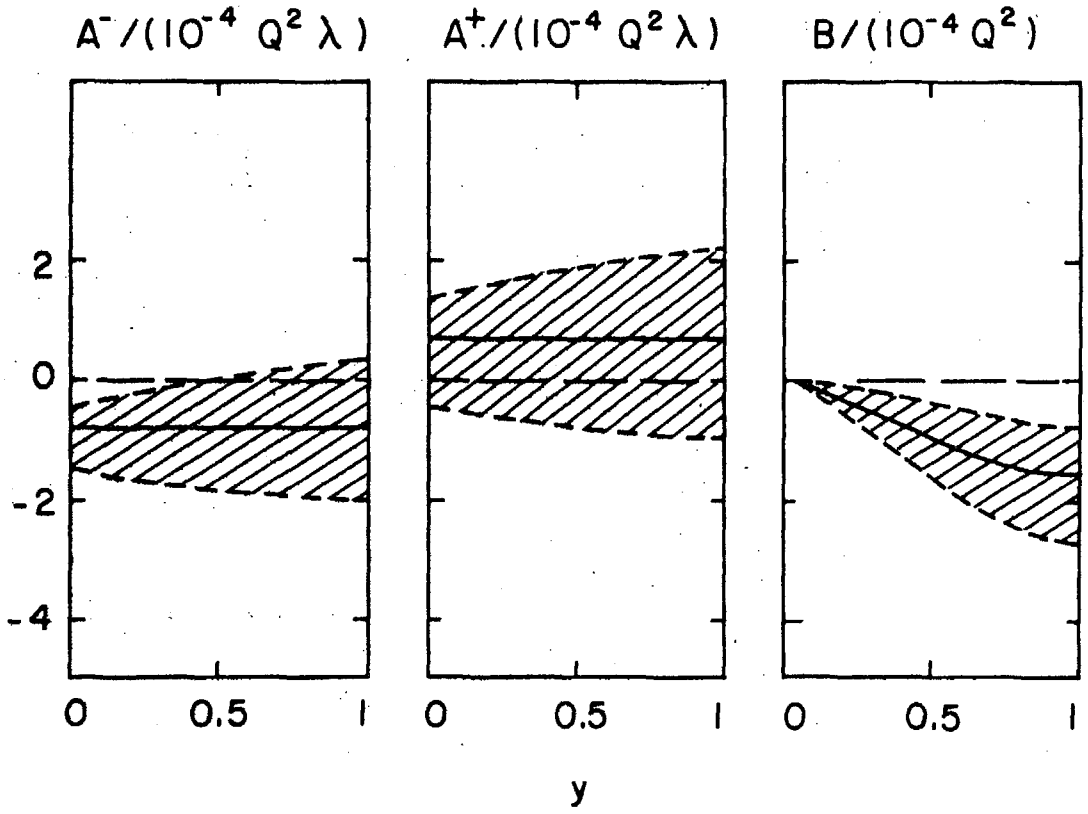

fig. 9

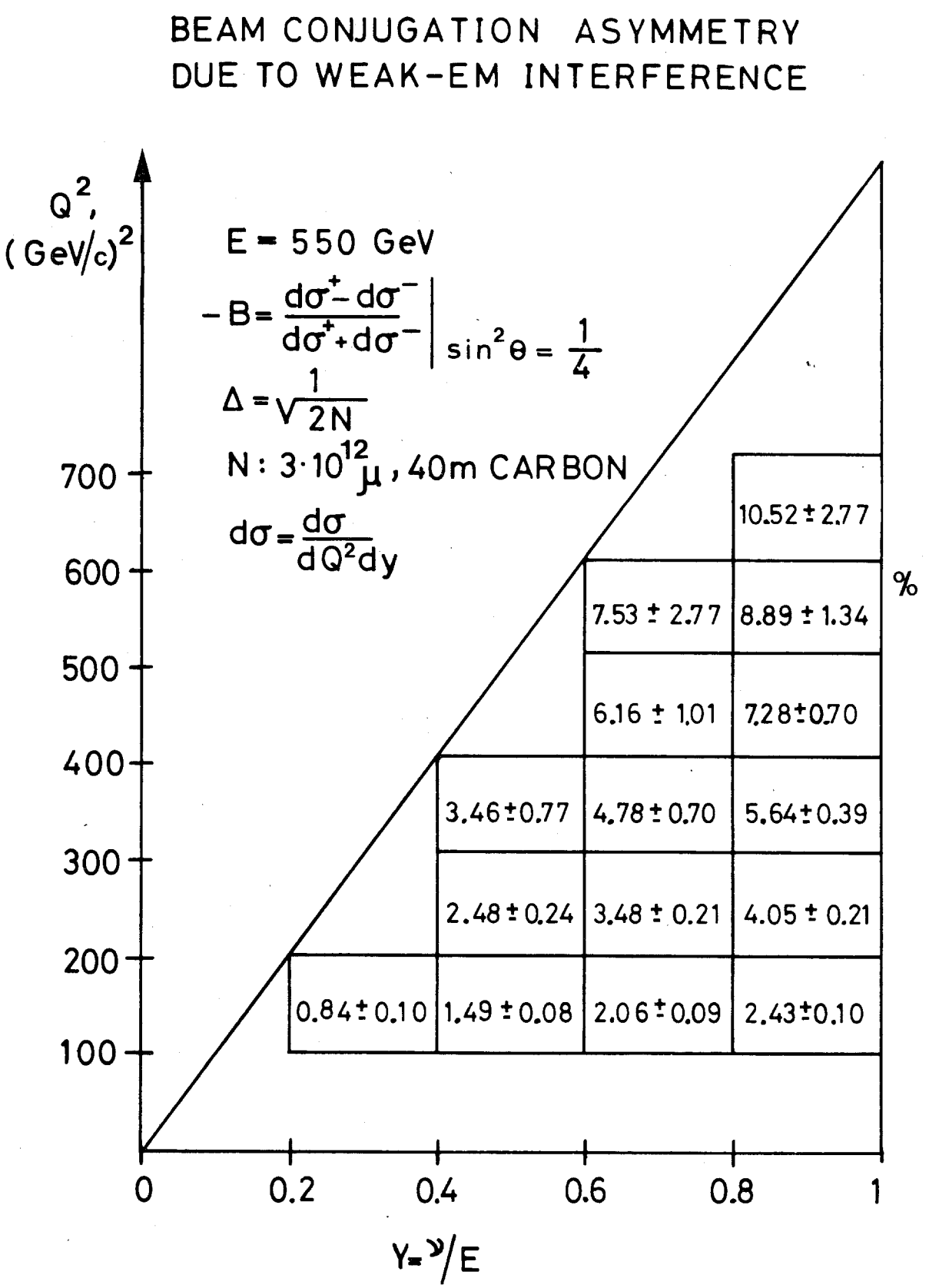
BEAM CONJUGATION ASYMMETRY
DUE TO WEAK-EM INTERFERENCE
Q^2, $(GeV/c)^2$
E = 550 GeV
$-B = \left| \frac{d\sigma^+ - d\sigma^-}{d\sigma^+ + d\sigma^-} \right|_{\sin^2\theta = \frac{1}{4}}$
$\Delta = \frac{1}{\sqrt{2N}}$
N : $3 \cdot 10^{12}\mu$, 40m CARBON
$d\sigma = \frac{d\sigma}{dQ^2 dy}$
700
600
500
400
300
200
100
10.52 ± 2.77
7.53 ± 2.77
8.89 ± 1.34
6.16 ± 1.01
7.28±0.70
3.46±0.77
4.78 ± 0.70
5.64±0.39
2.48 ± 0.24
3.48 ± 0.21
4.05 ± 0.21
0.84±0.10
1.49 ± 0.08
2.06±0.09
2.43±0.10
%
0
0.2
0.4
0.6
0.8
1
$Y = \nu/E$

fig. 10

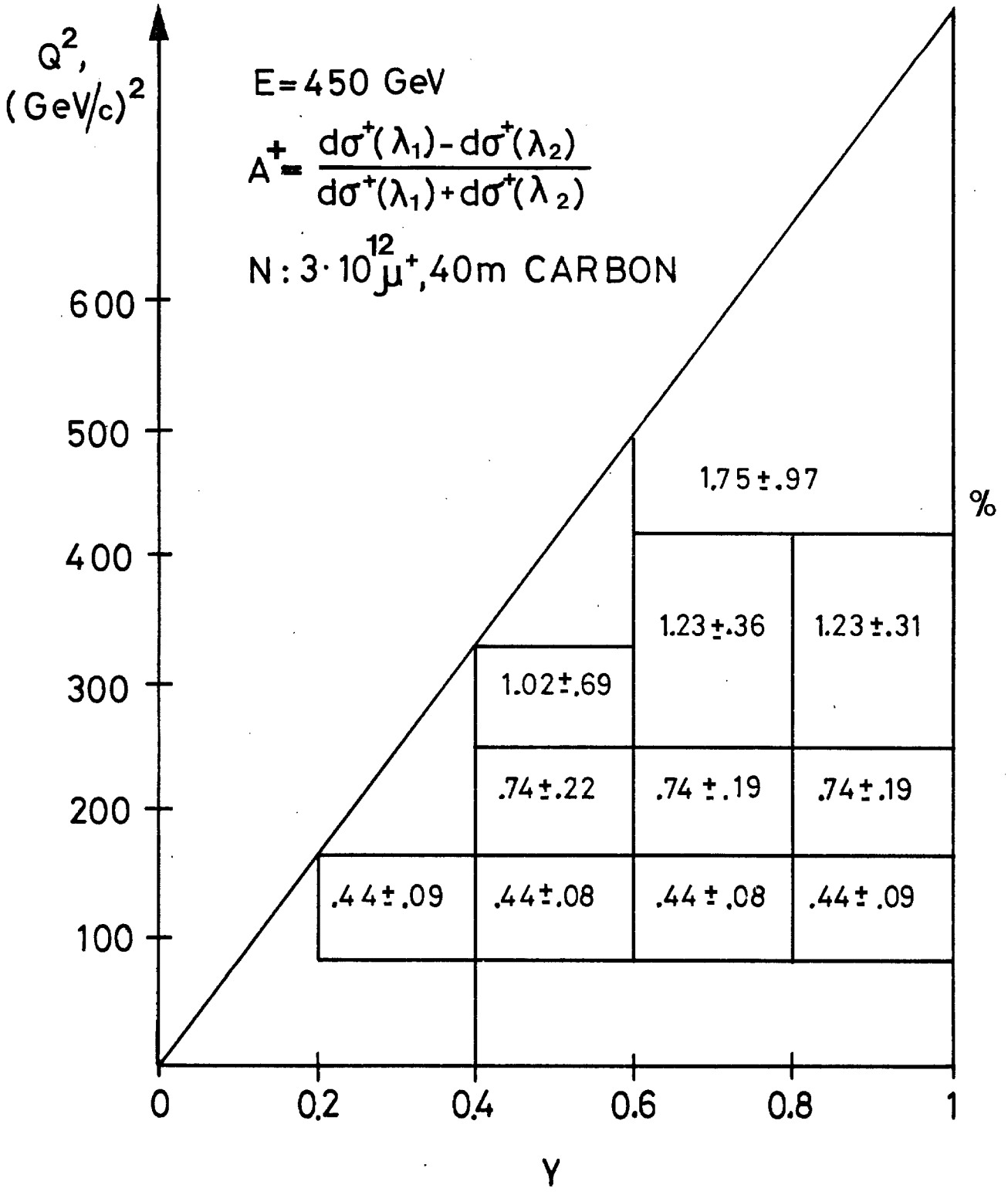
Q^2, $(GeV/c)^2$
E = 450 GeV
$A^{+-} = \frac{d\sigma^+(\lambda_1) - d\sigma^+(\lambda_2)}{d\sigma^+(\lambda_1) + d\sigma^+(\lambda_2)}$
N : $3 \cdot 10^{12}$ μ^+, 40m CARBON
600
500
400
300
200
100
1.75 ± .97
%
1.23 ± .36
1.23 ± .31
1.02 ± .69
.74 ± .22
.74 ± .19
.74 ± .19
.44 ± .09
.44 ± .08
.44 ± .08
.44 ± .09
0
0.2
0.4
0.6
0.8
1
Y

fig. 11

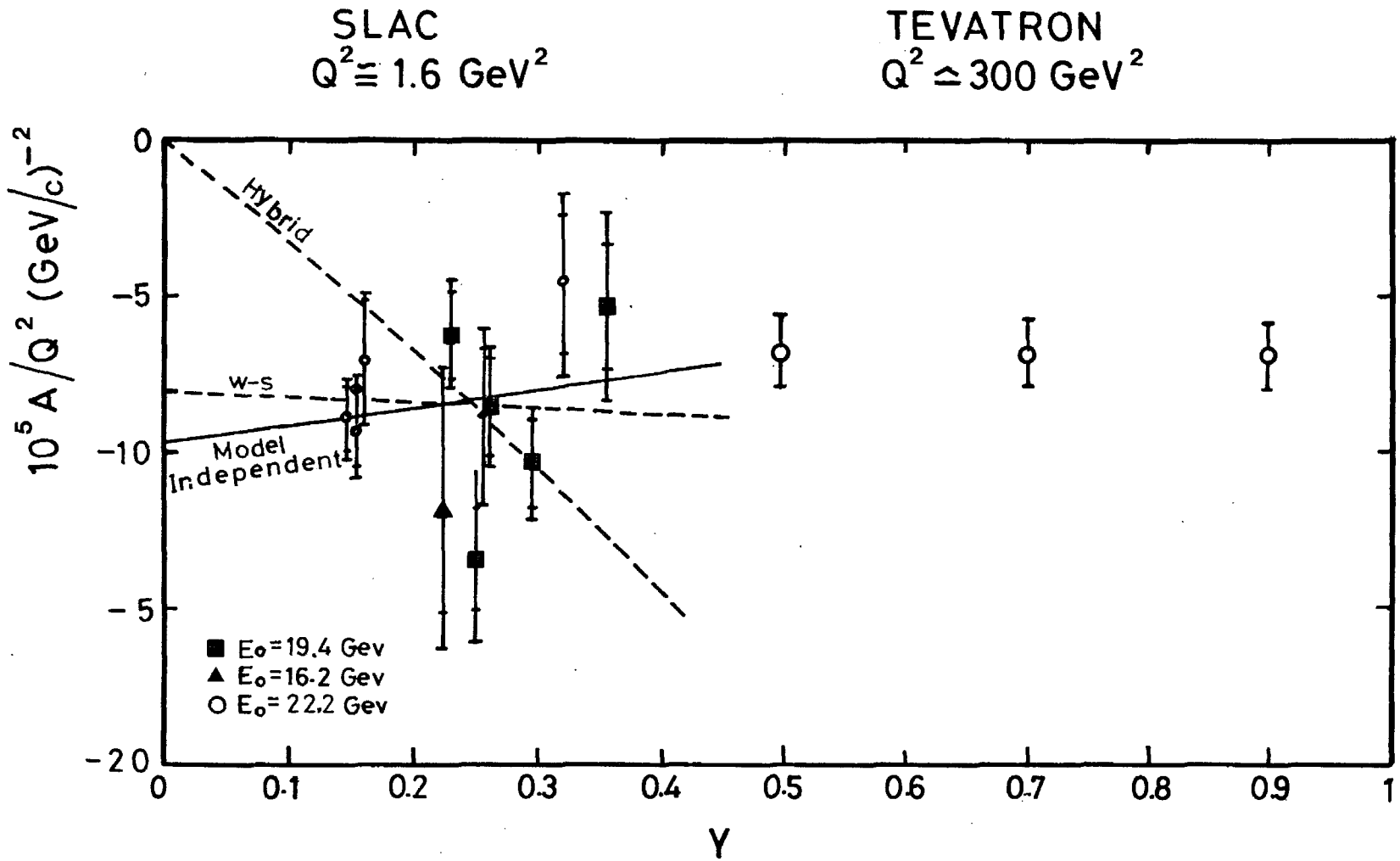
SLAC
$Q^2 \cong 1.6$ GeV^2
TEVATRON
$Q^2 \cong 300$ GeV^2
$10^5 A/Q^2$ (GeV/c)$^{-2}$
Hybrid
W-S
Model Independent
■ E_o=19.4 Gev
▲ E_o=16.2 Gev
○ E_o= 22.2 Gev
0
-5
-10
-5
-20
0
0.1
0.2
0.3
0.4
0.5
0.6
0.7
0.8
0.9
1
Y

fig. 12

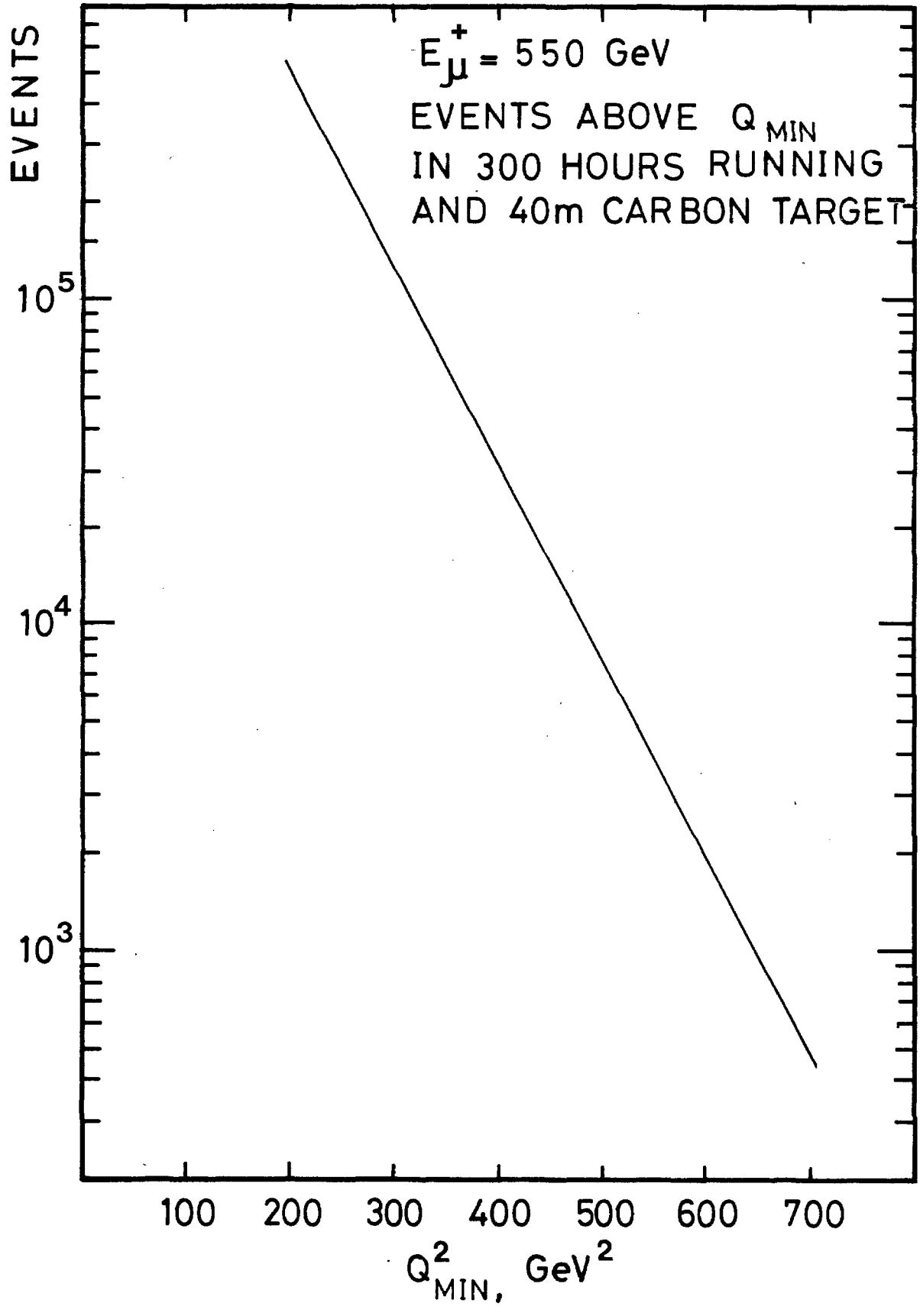
EVENTS
$E_\mu^+ = 550$ GeV
EVENTS ABOVE Q_{MIN}
IN 300 HOURS RUNNING
AND 40m CARBON TARGET
10^5
10^4
10^3
100
200
300
400
500
600
700
Q^2_{MIN}, GeV^2

fig. 13

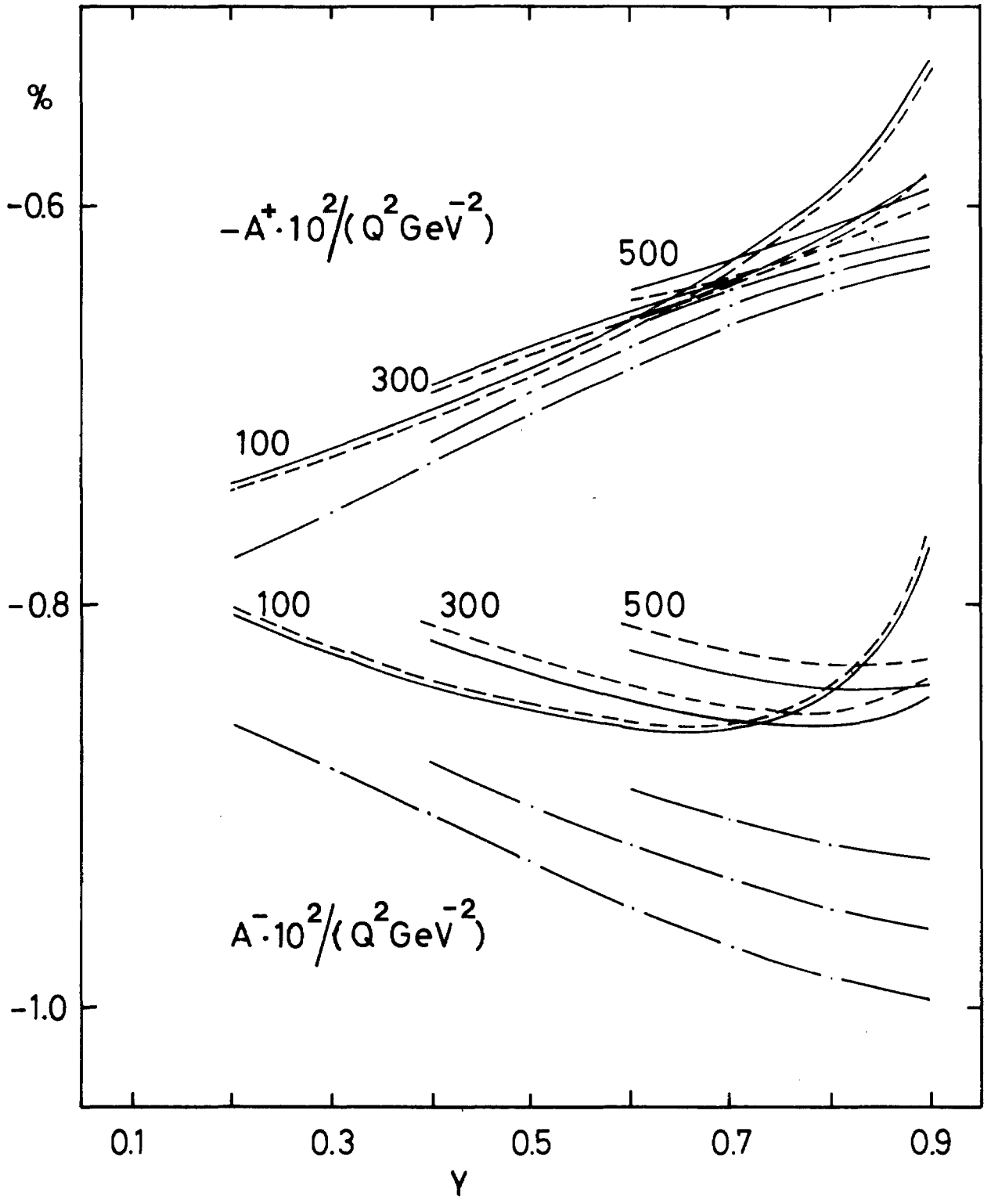
%
-0.6
-0.8
-1.0
$-A^{+}\cdot 10^{2}/(Q^{2}GeV^{-2})$
500
300
100
100
300
500
$A^{-}\cdot 10^{2}/(Q^{2}GeV^{-2})$
0.1
0.3
0.5
0.7
0.9
Y

fig. 14(a)

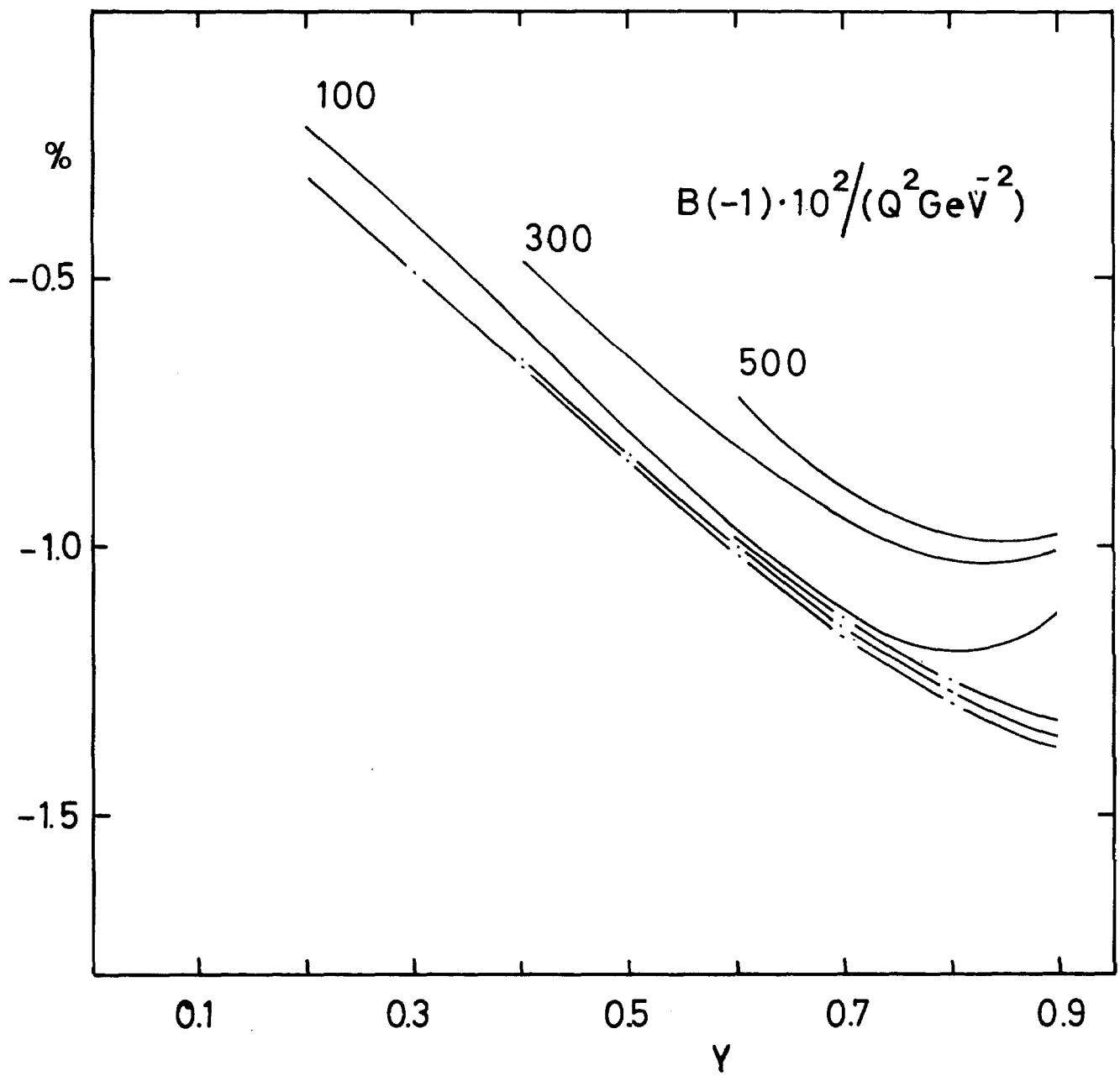

fig. 14(b)

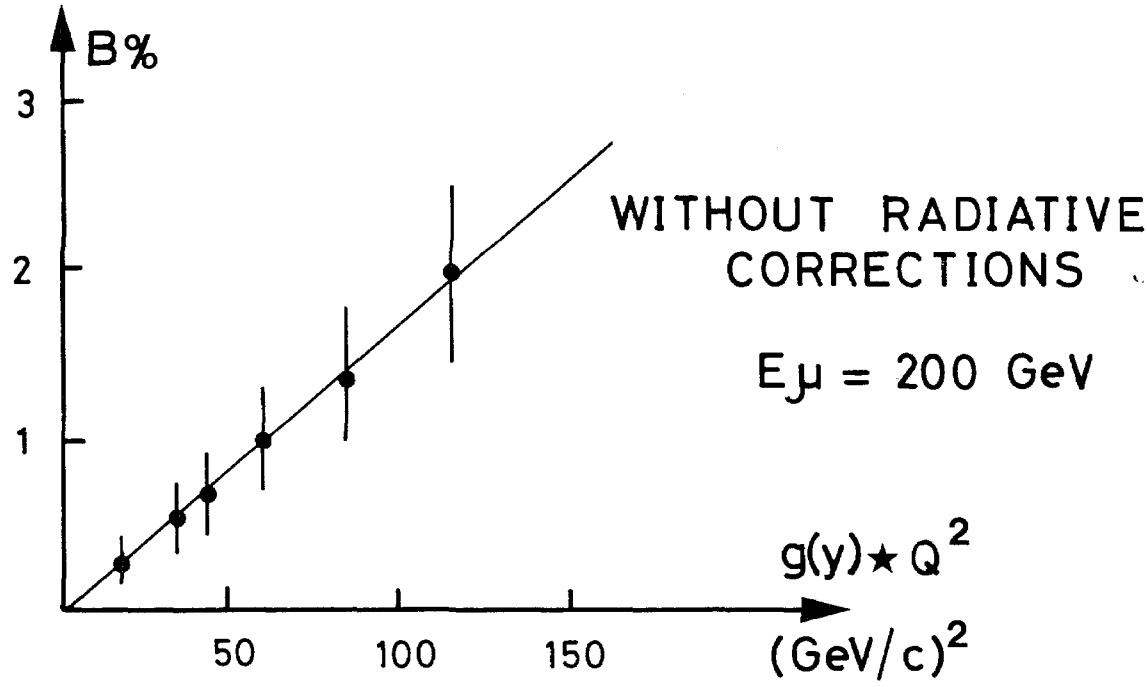
B%
3
2
1
WITHOUT RADIATIVE
CORRECTIONS
Eμ = 200 GeV
g(y)★ Q²
50
100
150
(GeV/c)²

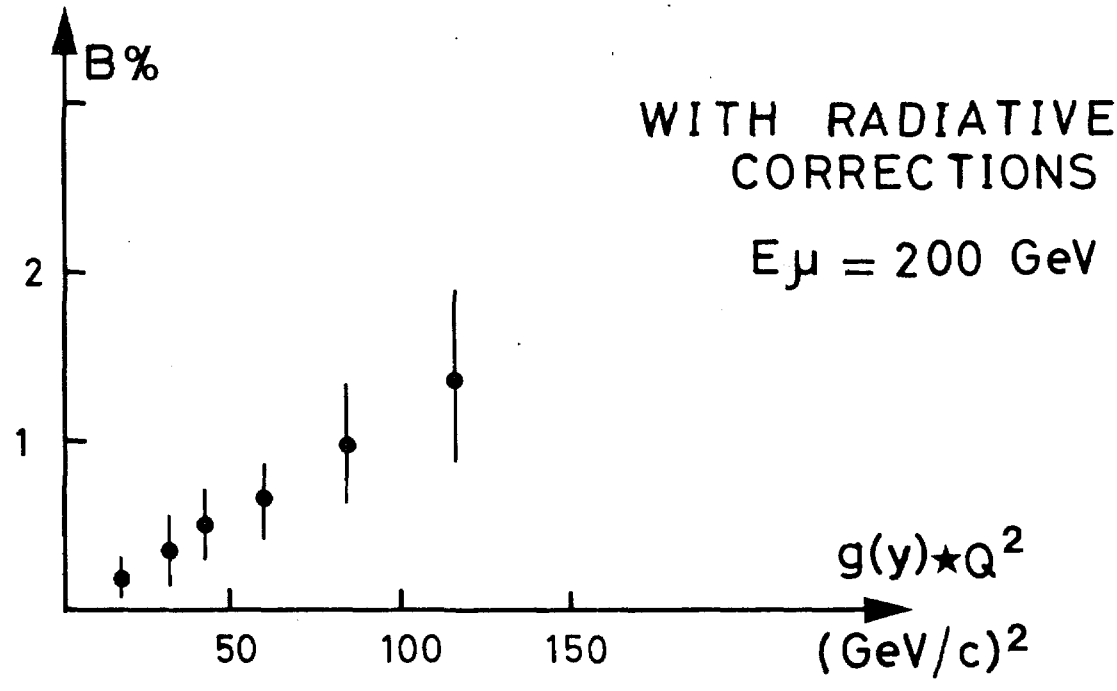
B%
2
1
WITH RADIATIVE
CORRECTIONS
Eμ = 200 GeV
g(y)★Q²
50
100
150
(GeV/c)²

fig. 15